supporting $C_{i^*j^*k} = 1$ to the node of the lower layer of (j^*, k) encoding $S_{i^*j^*k} = 1$.

(5) The promotion of request-proportional broadcasting by assigning uniform σ_i $(1 \le i \le I)$ to all the nodes of the upper layer of all sub-networks supporting that s_i broadcasts

$$\sigma_i = \begin{cases} B \times (R_i - A_i) & \text{if } R_i - A_i \ge 1 \\ 1 & \text{if } R_i - A_i < 1, R_i > 0 \\ 0 & \text{if } R_i = 0 \end{cases} \quad (3)$$

where B is a positive constant and A_i equals the number of sub-networks that exclusively promote broadcasting of s_i and have no lateral inhibition with other sub-networks.

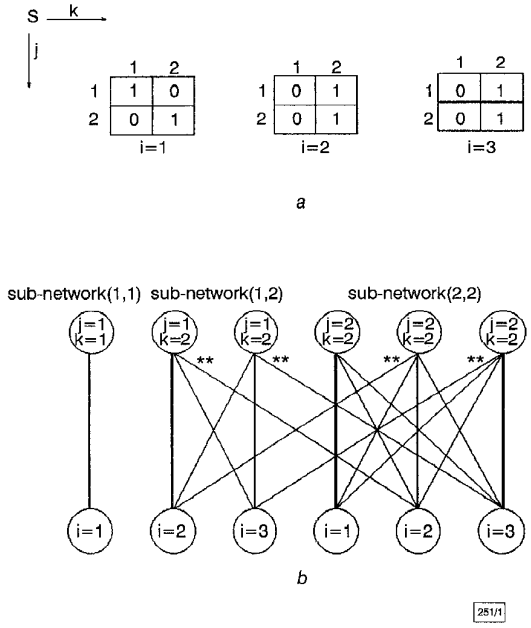

Fig. 1 *Sample SBS and corresponding ANN*

a Sample SBS ($I = 3$, $J = 2$, $K = 2$)
b Corresponding ANN

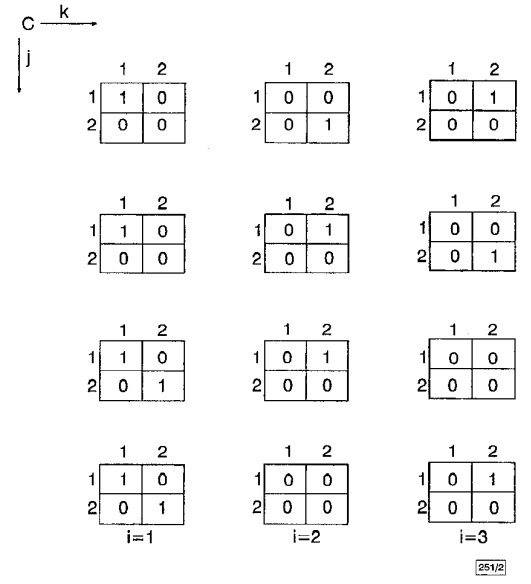

Fig. 2 *ANN solutions of sample SBS*

The ANN constructed for the sample SBS of Fig. 1*a* is illustrated in Fig. 1*b*. Sub-network (2, 1) is omitted as no satellite broadcasting to t_2 at T_1 exists. Positive and negative connections appear as bold and thin lines, respectively. The lateral inhibitory connections between sub-networks (1, 2) and (2, 2) are marked as **.

Test results: The SBS tests performed include the problems in [1] as well as more complex problems that have been randomly generated with $I \le 15$, $J \le 10$, $K \le 20$ and sparsity (proportion of zeros) of S not exceeding 60%.

The solution is provided by the active nodes of the ANN. From (iv), at most one node of the upper and one of the lower layer can be active in each sub-network (valid and correct broadcasting). Owing to maximal constraint satisfaction, the greatest possible number of active nodes of the upper layer is produced (optimal broadcasting). if more than one optimal solution exists, each is settled on by the ANN with roughly equal probability. If the communication task cannot be completed (i.e. (i) cannot be fulfilled for at least one s_i^*), the ANN solution is still valid while maximal broadcasting is accomplished from (ii). The number of updates required for ANN settling is affected by the problem complexity, namely the size of the largest sub-network (i, j) and the amount of lateral inhibition between sub-networks.

Fig. 2 shows the solutions produced by the ANN for the sample SBS of Fig. 1, where $B = 2$ is used in eqn. 3 and eight node activation updates are required for ANN settling. The first two instances of C depict the solutions for $R^T = [1\ 1\ 1]$; they constitute the two optimal solutions and each is settled upon with probability $p \simeq 0.5$. The third and fourth instances of C depict the solutions for $R^T = [2\ 1\ 0]$ and $R^T = [2\ 0\ 1]$, respectively; both constitute unique optimal solutions and are invariably settled upon. All instances of C are produced for $R^T = [2\ 1\ 1]$, a communication task that cannot be completed; the greatest possible number of communication requests is fulfilled and the solutions are settled on with $p \simeq 0.43$, 0.46, 0.04, 0.07, respectively; the preference for the first two solutions is due to the strength assignment in eqn. 3.

Conclusions: An artificial neural network employing problem decomposition and lateral inhibition has been utilised for solving the satellite broadcasting problem in parallel. The proposed solutions are valid (the problem constraints are satisfied), correct (the communication requests are fulfilled) and optimal (maximal broadcasting is accomplished).

© IEE 1998
6 May 1998
Electronics Letters Online No: 19981054

T. Tambouratzis (*Institute of Nuclear Technology - Radiation Protection, NCSR 'Demokritos', Aghia Paraskevi 153 10, Athens, Greece*)

References

1 ANSARI, N., and HOU, E.S.H.: 'A new method to optimize the satellite broadcasting schedules using the mean field annealing of a Hopfield neural network', *IEEE Trans. Neural Netw.*, 1995, **6**, pp. 470–483

2 FUNABIKI, N., and NISHIKAWA, S.: 'A binary Hopfield neural-network approach for satellite broadcast scheduling problems', *IEEE Trans. Neural Netw.*, 1997, **8**, pp. 441–445

3 SMOLENSKY, P.: 'Information processing in dynamical systems: Foundations of harmony theory' *in* RUMELHART, D.E., and J.L. McCLELLAND (Eds.): 'Parallel distributed processing: foundations, Vol.1' (MIT Press, Cambridge, MA, 1986) pp. 194–281

Solving maximum clique problem by cellular neural network

N.S. Şengör, M.E. Yalçın, Y. Çakır, M. Üçer, C. Güzeliş, F. Pekergin and Ö. Morgül

An approximate solution of an NP-hard graph theoretical problem, namely finding maximum clique, is presented using cellular neural networks. Like the existing energy descent optimising dynamics, the maximal cliques will be the stable states of cellular neural networks. To illustrate the performance of the method, the results will be compared with those of continuous Hopfield dynamics.

Introduction: Problems arising in fields as diverse as pattern recognition, computer vision, information processing etc. can be transformed into the maximum clique problem. Hence, it is of interest to develop methods to find exact and approximate solutions to the

maximum clique problem, which has many equivalent formulations as an integer programming problem or a continuous nonconvex optimisation problem. Owing to its simple formulation, the maximum independent set problem, which is equivalent to the maximum clique problem, is mainly considered. The method proposed in this Letter is based on the unconstrained quadratic 0-1 programming formulation given in [1], and is a local method with good approximation.

The maximum clique problem aims to find the largest clique in an undirected graph. The graph is assumed to have no loops, not more than one edge associated to a vertex pair, and at least one edge. A clique is a set of vertices in a graph such that every pair is connected by an edge. In a more formal way, this can be stated as follows: if $G = (V, E)$ is an undirected graph, where V is the set of vertices and E is the set of edges, a subset S of vertices is called a clique if the subgraph introduced by S is complete. A maximum clique of G is a clique of maximum cardinality. The solutions of the 0-1 optimisation problem defined with cost function $min(\mathbf{x}^T\mathbf{A}\mathbf{x} - \mathbf{e}^T\mathbf{x})$, $\mathbf{x} \in \{0, 1\}^n$, gives the maximal clique of G. Here $\mathbf{A}$ is the adjacency matrix of G and for $i, j = 1, 2, ..., n$, $a_{ij} = a_{ji} = 1$ iff $(v_i, v_j) \in E$ and $\mathbf{e} = (1, 1, ..., 1)^T$. Since G is an undirected graph and has no loops, it follows that $\mathbf{A}$ is a symmetric matrix with $a_{ii} = 0$ for $i = 1, 2, ..., n$. It is known that a point $\mathbf{x}^* \in \{0, 1\}^n$ is a discrete local minimum of $\mathbf{x}^T\mathbf{A}\mathbf{x} - \mathbf{e}^T\mathbf{x}$ iff $\mathbf{x}^s$, which is equal to $\mathbf{x}^*$, defines a maximal independent set for G [1]. The characteristic vector $\mathbf{x}^s \in \{0, 1\}^n$ is defined as follows: $x_i^s = 1$ if $v_i \in S$, $x_i^s = 0$ if $v_i \notin S$ for $i = 1, 2, ..., n$.

Several neural network models, which are mostly of the Hopfield type, have been proposed for the maximum clique problem [2, 3]. Even though the problem is discrete in nature, both discrete and continuous models of neural networks are used. The method proposed in this Letter is based on a continuous cellular neural network [CNN] [4], although the formulation is based on the 0-1 programing problem as stated above. The method given here is motivated by the piecewise linear dynamics of the CNN. Like most analogue neural network models, continuous relaxation is used for handling discrete variables and the original optimisation variables take discrete values as a function of these new variables. Since the cellular neural network minimises its quadratic energy function, the quadratic cost formulation of the maximum clique problem is chosen here. The maximum cliques will be the stable states of the CNN. It should be noted that, due to the nonregular structure of a given graph, the CNN used for approximating the maximum clique of the graph may be fully-connected and, furthermore, may possess a nonuniform connection weight pattern.

Cellular neural network formulation for maximum clique problem: The motivation of the proposed method is the completely stable dynamical behaviour of the CNN. It is well known that the dynamics of the CNN, given by the following state equations:

$$\dot{\mathbf{x}} = -\delta\mathbf{x} + \mathbf{W}\mathbf{f}(\mathbf{x}) + \mathbf{u} \quad f(x_k) = \frac{1}{2}(|x_k + 1| - |x_k - 1|) \quad 1 \le k \le n \quad (1)$$

where $\mathbf{x}$ and $\mathbf{u}$ are the state vector and input vector, respectively, minimise the related 'energy' function [4, 5] for the symmetric $\mathbf{W}$ matrix. This energy function is as follows:

$$E_{CNN}(\mathbf{x}) = -\frac{1}{2}\mathbf{f}^T(\mathbf{x})\mathbf{W}\mathbf{f}(\mathbf{x}) + \frac{1}{2}\mathbf{f}^T(\mathbf{x})\mathbf{f}(\mathbf{x}) - \mathbf{u}^T\mathbf{f}(\mathbf{x}) \quad (2)$$

For CNN formulation, the cost function for the maximum clique problem is redefined as given below:

$$E(\mathbf{x}) = \mathbf{x}^T\mathbf{A}\mathbf{x} - \mathbf{e}^T\mathbf{x} + \lambda(\mathbf{x}^T\mathbf{x} - \mathbf{e}^T\mathbf{x}) \quad (3)$$

Here, the last term is added to obtain binary steady-state outputs for the CNN. Since the stable states of the CNN are elements of $\{0, 1\}^n$, the unipolar binary variables $\mathbf{x} \in [0, 1]^n$ have to be transformed into bipolar ones. After defining new variable $\mathbf{y} := 2\mathbf{x}-\mathbf{e}$, the 'energy' function becomes

$$E_{CNN}(\mathbf{y}) = -\frac{1}{4}\mathbf{y}^T(\delta\mathbf{I}-\mathbf{A})\mathbf{y} + \frac{1}{4}(\delta+\lambda)\mathbf{y}^T\mathbf{y} - \frac{1}{2}\mathbf{e}^T(\mathbf{I}-\mathbf{A})\mathbf{y} \quad (4)$$

Here, the term $\mathbf{y}^T\delta\mathbf{y} - \mathbf{y}^T\delta\mathbf{y} = 0$ is added in order to obtain a dynamical representation similar to CNN which has non-zero self state feedback connection weights. The equation system governing the CNN dynamics after the change of variables and related with the energy function given in eqn. 4 will be as follows:

$$\dot{\mathbf{y}} = -\delta\mathbf{y} + \mathbf{W}f(\mathbf{y}) + \mathbf{u} \quad (5)$$

where $\mathbf{W} := [(\delta - \lambda)\mathbf{I} - \mathbf{A}]$, $\mathbf{u} := (\mathbf{I} - \mathbf{A})\mathbf{e}$. Thus, the defined weight matrix $\mathbf{W}$ is symmetric, since $\mathbf{A}$ is the adjacency matrix of the considered undirected graph. The diagonal of $\mathbf{W}$ is positive, because δ is positive valued while λ is negative valued. In the CNN formulation stated above, $\mathbf{A}$ is used in defining the connection weights in a fully connected CNN. As stated in [4, 5], the CNN is completely stable for a symmetric weight matrix $\mathbf{W}$ and the stable equilibrium points of eqn. 5 are the minimums of the 'energy' function in eqn. 4. Solving the differential equation eqn. 5 coincides with finding a maximal clique of G.

Table 1: Average clique sizes found for 100- and 400- graphs with densities of 0.25, 0.50 and 0.75

$\|V\|$	Density	Overall average		Average over bests among 5 runs		Average over bests among 10 runs	
		CHD	CNN	CHD	CNN	CHD	CNN
100	0.25	4.48	4.176	4.58	4.84	4.62	5.14
	0.50	7.38	7.096	7.59	8.07	7.66	8.32
	0.75	13.87	13.562	14.24	14.69	14.40	15.18
400	0.25	5.53	5.099	5.96	5.91	6.08	6.046
	0.50	9.24	8.866	10.03	9.823	10.30	8.867
	0.75	18.79	18.116	19.93	19.606	20.28	20.133

Experimental results: The performance of the CNN is illustrated on random graphs of various vertex sizes and densities. Average maximum cliques, where the averages are taken over the test graphs generated with the same characteristics, i.e. the vertex size and densities, are considered as the primary performance measure. This performance provides an indirect comparison of the results obtained here with those reported for continuous Hopfield dynamics [CHD]. Another performance measure is also considered, in which the averages are computed for the same test sets but taking into account only the best results obtained on each graph in five and ten independent runs of the CNN with random initial conditions. This measure shows the ability of the method to find different search directions when it is started from different initial points. The experimental results are summarised in Table 1 for $\lambda = -0.5$, $\delta = 0.01$ and the initial conditions chosen randomly near the origin. Further experimental results are given in [6], where comparison with saturated linear dynamics is also considered.

Conclusion: In this Letter a method based on cellular neural networks is introduced to approximate the solution of the maximum clique problem. The quadratic cost formulation of the maximum clique problem is considered here to exploit the quadratic energy function minimisation capability of the CNN. The adjacency matrix of the considered problem is used in defining the weighted connections in a fully connected CNN. The stable equilibrium points of the CNN are the minimums of its energy function, which is equated to the quadratic cost function of the maximum clique problem. Solving the differential equation system defining the cellular neural network gives one of the maximal cliques as the local minimum of the related energy function.

© IEE 1998
1 June 1998
Electronics Letters Online No: 19981026

N.S. Şengör, M.E. Yalçın, Y. Çakır, M. Üçer and C. Güzeliş (*İstanbul Technical University, Maslak 80626, İstanbul, Turkey*)

F. Pekergin (*LIPN - Université Paris-Nord, 93430-Villetaneuse, France*)

Ö. Morgül (*Bilkent University, Bilkent, Ankara, Turkey*)

References

1 PARDALOS, P.M., and ROGERS, G.P.: 'A branch and bound algorithm for the maximum clique problem', *Comput. Oper. Res.*, 1992, **19**, (5), pp. 363–375

2 JAGOTA, A.: 'Approximating maximum clique with a Hopfield network', *IEEE Trans. Neural Netw.*, 1995, **6**, (3), pp. 724–735

3 FUNABIKI, N., TAKEFUJI, Y., and LEE, K.C.: 'A neural network model for finding a near maximum clique', *Parallel Distrib. Comput.*, 1992, **14**, pp. 340–344

4 CHUA, L.O., and YANG, L.: 'Cellular neural networks: Theory', *IEEE Trans. Circuits Syst.*, 1988, **35**, pp. 1257–1272

5 WU, C.W., and CHUA, L.O.: 'A more rigorous proof of complete stability of cellular neural networks', *IEEE Trans. Circuits Syst.*, 1997, **44**, pp. 370–371
6 ŞENGÖR, N.S., YALÇIN, M.E., ÇAKIR, Y., ÜÇER, M., GÜZELIŞ, C., PEKERGIN, F., and MORGÜL, Ö: 'An application of cellular neural network: Maximum clique problem'. 1998 Fifth IEEE Int. Workshop on Cellular Neural Networks and Their Appl. Proc., London, 1998, pp. 208–211

160Gbit/s WDM transmission experiment using four 40Gbit/s optical duobinary channels

K. Yonenaga, M. Yoneyama, Y. Miyamoto, K. Hagimoto and K. Noguchi

Four-channel multiplexed 40Gbit/s optical duobinary signals are successfully transmitted over a 100km dispersion-shifted fibre for the first time. 40Gbit/s based four-channel WDM transmission without individual channel dispersion compensation was achieved by virtue of the high dispersion tolerance of the optical duobinary signal.

Introduction: To construct ultra-high-capacity networks, high-speed optical transmission technologies are very important. The transmission capacity of a single carrier has recently reached 40Gbit/s in electrical time-division multiplexing systems [1, 2]. In such high-speed optical transmission systems, the tolerable dispersion range is very small and precise dispersion control is indispensable [3]. For expansion of the dispersion range, the optical duobinary transmission technique is promising [4], and has been demonstrated in a 40Gbit/s transmission system [5]. The optical duobinary technique is also suitable for WDM transmission systems that multiplex high-speed channels because of the high dispersion tolerance and high frequency-utilisation efficiency.

This Letter demonstrates 160Gbit/s WDM transmission using four-channel multiplexed 40Gbit/s optical duobinary signals over a 100km dispersion-shifted fibre (DSF). The optical duobinary technique expands the usable bandwidth and transmission distance in 40 Gbit/s based WDM systems without individual channel dispersion compensation or dispersion slope compensation.

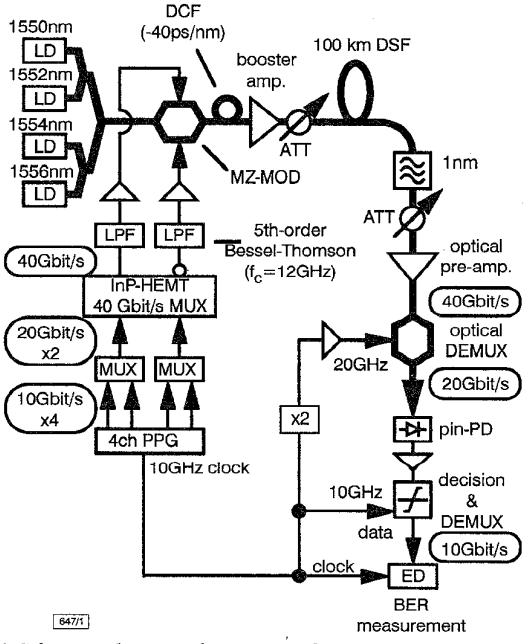

Fig. 1 *Schematic diagram of experimental setup*

Experiments: Fig. 1 shows a schematic diagram of our experimental setup. A 2^7–1 pseudo-random binary sequence (PRBS) 40Gbit/s signal was generated by an InP-HEMT selector IC [6] from two 2^7–1 PRBS 20Gbit/s signals. The 40Gbit/s binary signals (data and complementary data) were converted to duobinary signals by using fifth-order Bessel-Thomson lowpass filters (LPFs), with a 3dB bandwidth of 12GHz, as a duobinary filter. The duobinary signals were supplied to two electrodes of a push-pull type $LiNbO_3$ Mach-Zehnder (MZ) modulator with an electrical 3dB bandwidth of 30GHz [7]. A high-power driver with 20GHz bandwidth was used for 40Gbit/s duobinary modulation. The driving voltage was ~$5V_{p-p}$. To realise good eye-opening of the 40Gbit/s optical duobinary signal, this voltage was slightly higher than the half-wavelength voltage of the MZ modulator, 3.9V.

Four optical carriers, whose wavelengths ranged from 1550 to 1556nm, were simultaneously modulated by the push-pull type MZ modulator. The zero-dispersion wavelength of the 100km transmission fibre was 1540nm and its dispersion was 0.66ps/nm/km at 1550nm. To reduce the total dispersion and to decorrelate the four-channel optical signals, a short dispersion compensation fibre (DCF) preceded the transmission fibre. A total power of +13dBm was launched into the transmission fibre. A 1nm optical bandpass filter (OBPF) was used for WDM channel selection, and the selected signal was optically demultiplexed into a 20Gbit/s return-to-zero optical signal with an MZ modulator. The 20Gbit/s optical signal was detected by a *pin* photodiode and demultiplexed into a 10Gbit/s signal by a decision circuit.

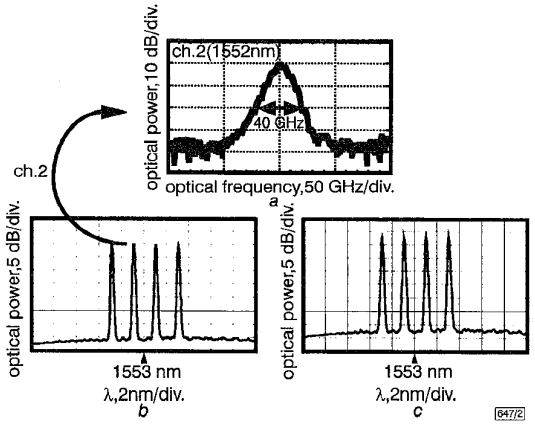

Fig. 2 *Optical spectra of 40Gbit/s optical duobinary signal and four-channel WDM signal*

a 40Gbit/s optical duobinary signal spectrum
b WDM spectrum before transmission (0km)
c WDM spectrum after transmission (100km); Pin = +13dBm

Fig. 2 shows the optical spectra of the 40Gbit/s optical duobinary signal and the four-channel WDM signal. Fig. 2*b* shows the WDM spectrum before transmission. The carrier wavelengths were 1550nm (channel 1), 1552nm (channel 2), 1554nm (channel 3) and 1556nm (channel 4). All channels were in the anomalous dispersion region, i.e. apart from the zero-dispersion wavelength of the transmission fibre (1540nm). Fig. 2*c* shows the WDM spectrum after 100km transmission. No four-wave mixing was observed because of the large dispersion in the signal wavelength region. Fig. 2*a* shows the expanded spectrum of the 40Gbit/s optical duobinary signal (channel 2). The spectrum shows characteristics of narrow bandwidth and a suppressed carrier, basic attributes of an optical duobinary signal.

Fig. 3 shows the results of 100km DSF transmission. The 40Gbit/s eye-diagrams, shown in Fig. 3*a*, were observed at the input of the optical demultiplexer. All channels have good eye-opening even though individualchannel dispersion compensation was not used because of the high-dispersion tolerance of the optical duobinary signal. Fig. 3*b* shows the average bit error rate (BER) performances for all channels. The BERS for the four demultiplexed time slots were individually measured by adjusting the clock phase. Receiver sensitivity difference between the four demultiplexed time slots was < 1dB for all channels. The DCF (–40ps/nm), which was inserted to reduce the total dispersion and to decorrelate the four-channel optical signals, was not used in back-to-back BER measurements. Before transmission, the receiver sensitivity at a BER of 10^{-9} was –23.2dBm for all channels. After 100 km transmission, the sensitivities for channels 1, 2, 3, and 4 were –23.8, –24.6, –24.8 and –25.2dBm, respectively. It is